SUPPLEMENTAL MATERIAL

Supplemental Methods

Reagents

18 cm IPGstrips (pH range 4-7 and 6-11), agarose NA, and CyDyes were purchased from GE healthcare. Bis-acrylamide from BioRad Laboratories. Alkaline Phosphatase (Calf Intestinal Phosphatase, CIP) from New England Biolabs. Protease inhibitors Complete from Roche. Mark 12 (unstained) and Seeblue (prestained) molecular weight markers, precast NuPAGE (4-12% BisTricine) and Blu Native BN-PAGE gels and PVDF membrane (immobilon, Milllipore) from Invitrogen. The anti-ATP synthase beta subunit antibody was purchased from MitoSciences (MS503, mouse, monoclonal). All other chemicals were purchased from Fischer Bioreagents, and were of the highest analytical grade.

Workflow

Supplementary Figure 6 describes the experimental strategies used in the present study. Altered proteins detected by spot density were identified using tandem mass spectrometry (MS/MS or tandem MS). Changes in the phosphorylation status of ATPβ and other proteins were monitored using a modified version of the protocol defined by Raggiaschi et al.[1, 2]. The dephosphorylated pool used here in place of the internal standard should be common to both samples conditions, at least as far as phosphorylation status is concerned (see below). Phospho-peptide enrichment with IMAC was used in combination with MS/MS to improve identification of the exact phosphorylated amino acid residues. Finally, functional assays were used to characterize complex V activity and assembly along with the determination of respiratory control index in isolated mitochondria.

Animal Model

Five animals were paced from the right atrium for six weeks at ~200 bpm (DHF); whereas the remaining four dogs were subjected to three weeks of atrial pacing (dyssynchrony) followed by three weeks of bi-ventricular tachypacing at the same rate (CRT) as described in[3]. Left bundle branch block (LBBB) was confirmed by intra-cardiac electrograms, with surface QRS widening from 50±7 to 104±7 ms ($p<0.001$). Bi-ventricular pacing was achieved by simultaneous lateral epicardial and right ventricular antero-apical free wall stimulation. At terminal study the hearts were extracted under cold cardioplegia, dissected into endocardial and mid/epicardial segments from the septum (i.e. LV and RV septum) and LV lateral wall, and frozen in liquid nitrogen. Tissue samples obtained from the upper third of the LV lateral wall were used in the present study.

Mitochondria Fractions Preparation

The protocol was designed to optimize reproducibility, minimize contamination from other subproteomes (e.g. myofilaments), and maximize protein recovery. Samples were kept on ice throughout the entire process to minimize artifactual protein modifications. Mitochondrial protein enrichment and myofilament contamination were monitored, along with the separation (Supplementary Figure 7). Briefly, frozen heart tissues (typically 500 mg) were crushed into a mortar filled with liquid nitrogen by means of a ceramic pestle. All of the following steps were performed in ice to prevent artefact protein degradation. Frozen tissue crumbs were transferred in a glass homogenizer filled with ice-cold H-buffer (220 mM mannitol, 70 mM Sucrose, 20 mM Hepes, pH 7.4) and briefly homogenized. Tissue homogenates were filtered through a 100 μm filter to remove connective tissues and collect

intact cardiac myocytes. The filtrate was centrifuged (1100 rcf, 5 min, 4 °C) and rinsed with ice-cold H-buffer four times. Supernatants were collected, and pellets discarded (cell debris, nuclei, and intact cells). Mitochondria were next "washed" from membranes and broken mitochondria by centrifuging three times at increasing centrifuge fields (7000, 18000 and 20000 rcf, 15 min, 4° C) and re-suspending the pellet in half of the volume after each centrifugation. Two further centrifugation steps (3000 rcf, 3 min, 4°C) were required to remove remnant myofilaments; supernatants were collected and finally centrifuged at high speed (20000, 20 min, 4°C) to pellet the purified mitochondria. Pellets were re-suspended in 100 µL H-buffer, gently, by pipetting up and down few times. 1 µL of the suspension was transferred into a 96 multiwell plate (flat bottom, costar) and diluted in 20 µL of 1% SDS, 5 % ASB 14 and protease inhibitor complete, in triplicate. A BSA (sigma, 2 mg/ml in the same buffer) standard curve was used to assay for protein quantity after 30 min incubation at 37°C (BCA, Pierce). Protein concentration was calculated, and mitochondrial suspensions were divided accordingly into 100 µg aliquots, and then flash frozen in liquid nitrogen for storage at -80°C. Mitochondrial protein enrichment and myofilament protein contamination was tested along with the purification process as displayed in Supplementary Figure 7.

Two-dimensional Gel Electrophoresis

Optimal resolution for basic mitochondrial proteins was achieved using the improved protocol developed by our laboratory[4]. The second dimension (SDS-PAGE) was run using 10% bis-tris gels with 2(n-morpholino) ethansulfonic acid (MES) running buffer[5]. Gel slabs were subsequently silver stained according to Shevchenko[6]. Sample pellets were

thawed and centrifuged (20000 rcf, 20 min, 4°C) and supernatant (H-buffer) discarded. 5% amidosulfobetaine-14 (ASB-14, Calbiochem) was added to the sample to solubilize membrane proteins prior to dilution in isoelectric focusing (IEF) re-hydration buffer (8 mol/L urea, 2.5 mol/L thiourea, 4% w/v 3-[3-cholamidopropyl]-1-propane-sulfonate [CHAPS], 0.5% ampholytes, 50 mmol/L DTT, 1% HED, and 0.01% w/v bromophenol blue). IEF was carried out using a Protean® IEF cell (Bio-Rad). Immobilized pH gradient (IPG) Strips (18 cm pH 4-7 linear gradients) were actively rehydrated with the sample (150 µg of protein in 350 µL IEF buffer) at 50 V for 12 hrs, followed by a rapid voltage ramping consisting of 1 hr each at 300, 600, and 1000 V, followed by 10000 V for 45 kVh at 20°C. For pH 6-11 IPG strips, IEF strips were passively rehydrated before focusing (10 hrs). Protein samples were added to rehydration buffer to give a final protein concentration of 1 mg/mL, and applied by paper bridge-loading as described in[4]. Proteins were separated in the second dimension by 10% Bis-Tris SDS-PAGE, using a MES running buffer (45 mmol/L [2-(N-morpholino) ethane sulfonic acid] or MES, 50 mmol/L Tris base, 0.1% SDS, 0.8 mmol/L EDTA, pH 7.3) as described previously[5]. IPG strips were reduced and alkylated for 20 min each, respectively using 1% (w/v) DTT and 4% (w/v) iodoacetamide in equilibration buffer (50 mmol/L Tris-HCl, pH 8.8, 6 mol/L urea, 30% v/v glycerol, 9% w/v SDS). IEF strips were rinsed briefly with MES running buffer, the excess of liquid was gently removed with a paper tissue, and the strips were loaded onto the 10% Bis-Tris SDS-PAGE gels. Strips were sealed using agarose sealing solution (50 mmol/L MES, 0.5% Agarose NA, 0.1% w/v SDS, bromophenol blue). Gels were run overnight on a Protean® II XL system (Bio-Rad) at 90 V. Gels were silver stained according to the protocol of

Shevchenko et al.[6]. Differential display analysis was performed using Progenesis (Nonlinear Dynamics, NC, US).

Immunoblotting

Proteins were transferred to PVDF in transfer buffer at 100 V for 1 hour in ice. Membrane were stained with Direct Blue 71 (Sigma), and images recorded for subsequent luminescent signal normalization. Membranes were then blocked overnight using Western Blocking Reagent (Roche); and incubated with 0.2 μg/mL anti-ATP synthase beta subunit antibody mouse IgG monoclonal (MS503, MitoSciences) in Tris-buffered saline completed with Tween 20 (TBS-T: 100 mmol/L Tris-Cl, 0.9% (w/v) NaCl, 0.1% (v/v) Tween 20) under gentle agitation for 1 hr, and then incubated with 0.03 μg/mL alkaline phosphatase-conjugated AffiniPure Goat Anti-Mouse (Jackson ImmunoResearch) in TBS-T under gentle agitation for 1 hr. For ATP synthase delta 2D-WB a rabbit-polyclonal antibody was used (anti-ATP5D, Atlas/Sigma Prestige, 0.05 μg/mL in TBS-T). In this case a alkaline phosphatase-conjugated AffiniPure Donkey Anti-Rabbit (Jackson ImmunoResearch) secondary antibody was also used. Chemiluminescent signal was produced using Immun-Star AP substrate pack (BioRad Laboratories) and luminescence was detected with scientific imaging film (Kodak).

Image Analysis and Quantification

Gel images were digitized at 200-300 dpi using a Epson Expression 10000XL device (Epson Electronics America, CA, USA). Protein spots were then quantified and matched with other gels using Progenesis Workstation 2005 software (NonlinearDynamics, New

Castle-upon-Tyne, UK). Composite images of each treatment group were normalized by means of a total spot intensity comparison between sample groups. Quantified spot changes were within the linear range of silver stain. The same platform was used to acquire and analyze densitometry data generated through western blotting analysis. In this case, the luminescent signal generated by each sample band and recorded on the imaging film was normalized against the density of the correspondent lane stained with the general protein staining DB71.

Protein identification by Mass Spectrometry

Protein spots were excised from fresh gels, and destained according to a modified protocol of Gharahdaghi et al. [7]. Proteins were digested in 25 mmol/L ammonium bicarbonate, pH 8.0 completed with 10 μg/mL sequencing grade modified porcine trypsin (Promega), for 16-24 h at 37ºC. Peptides were extracted twice with 50 μL of acetonitrile (ACN) and 25 mmol/L ammonium bicarbonate 1:1 v/v for 60 min and then dried under vacuum. Tryptic peptides were reconstituted in 3 μL of 50% ACN/0.1% TFA and analyzed by electrospray ionization (ESI) MS/MS LCQ Deca XP Plus mass spectrometer (ThermoFinnigan, San Jose, California), as described previously[8].

Data-dependent acquisition was used to obtain both a survey spectrum along with several MS/MS spectra for multiply charged precursor ions present in each sample. MS/MS spectra were processed by baseline subtraction, and de-convoluted using Mascot wizard. Database searching was performed using Mascot wizard (www.matrixscience.com) using the "other-mammalian" sub-database of NCBInr protein databases. FASTA sequences were blasted against Swissprot protein database through the proteomics tool Expasy Blast

(http://www.expasy.ch/tools/blast/) to further reduce protein redundancy. The number of unique peptides assigned by Mascot search and retrieval system is also listed for each protein. The Mowse score[9] provided by the software was manually recalculated (Corrected Mowse) summing unique peptides as defined in[10]. Observed and theoretical isoelectric point (pI) and molecular weight (MW) values for identified proteins are given; bold font is used for observed values that differ significantly from the theoretical ones ($\Delta pI \geq 1$ pH unit; $\Delta MW \geq 10$ kDa). These parameters were used to assign protein identities when ambiguous IDs were retrieved by Mascot.

Phosphopeptide Analysis by Immobilized Metal Affinity Chromatography (IMAC)

Phosphopeptides were eluted to a C18 pre-column and analyzed by nanoflow HPLC/micro-ESI MS/MS via data-dependent analysis on an LCQ Deca XP Plus mass spectrometer (ThermoFinnigan, San Jose, California). Peptide identification was performed by searching the raw MS/MS spectra against the ATPβ sequence (NCBI gi|73968432) using Bioworks 3.1 (ThermoFinnigan).

ATPβ De-phosphorylation Assay

Mitochondrial pellets were re-suspended in 1% (w/v) SDS and 5% (w/v) ASB14 completed with protease inhibitor cocktail Complete ™, and then pooled in three groups: DHF pool, CRT pool and DHF+CRT pool, each mixed with equal protein quantities. The latter pool (alkaline phopsphatase or AP pool) was then treated with alkaline phosphatase (CIP, New England Biolabs) overnight at 37°C. On the following day the pool samples were solubilized in CHAPS buffer and labelled with CyDyes (Cy3, Cy5 and Cy2 respectively)

for 20 minutes at room temperature. The labelling reaction was stopped by adding 20 mM Lysine to the samples. Samples were flash frozen or diluted in IEF buffer for two-dimensional electrophoresis. DHF and CRT pools were alternatively labelled with either Cy3 and Cy5 (dye swapping) to prevent artefact variations due to dye bias.

Blue Native PAGE (BN-PAGE)

Blue Native gel electrophoresis was performed using pre-cast native gels (Invitrogen) according to manufacturer's instructions. Briefly, mitochondrial suspensions were thawed, centrifuged to remove the H-buffer, and diluted in blue native sample buffer completed with 2% Lauryl Maltoside, and incubated 30 min in ice. Samples were then centrifuged (20000 rcf, 30 min, 4°C) to remove insoluble material. Supernatants were completed with 5% Colloidal Coomassie Blue G-250 (0.25% final concentration) and separated for 1 hr 30 min at 150 V. Protein complexes were subsequently blotted onto PVDF as described in immunoblotting section.

In-gel ATPase Activity

The procedure described in previous section (BN-PAGE) was also followed to separate mitochondrial complexes for further determination of complex V activity as described by Bisetto et al.[11]. Briefly, BN-PAGE gels were equilibrated for two hours in equilibration buffer (33 mM Tris, 285 mM Glycine, 13 mM $MgSO_4$). After equilibration the gels were incubated in fresh equilibration buffer completed with 8.8 mM ATP and 0.2% w/v $Pb(NO_3)_2$, for 2 hours at room temperature. In these conditions the ATP-ase activity of F_1/F_o hydrolyses ATP to ADP and inorganic phosphate. Phosphate forms a white insoluble

lead salt that precipitates locally and originates a white band whose density is proportional to ATP-synthase activity on the separated F_1/F_o bands. Densitometric analysis was performed using a dark background screen and the values were normalized vs. the coomassie G250 signal of complex V band after separation.

Measurement of Oxygen Consumption in Isolated Mitochondria

Mitochondria were isolated from the left ventricles of sham, DHF and CRT dogs. Ventricles were placed in ice-cold isolation buffer (containing 225 mM mannitol, 75 mM sucrose, 1 mM EGTA, 20 mM Hepes, 0.2% BSA, pH 7.4), then rapidly minced and homogenized using the Polytron homogenizer at low speed. The homogenate was centrifuged at 500 g for 10 minutes at 4°C (Sorvall, SS34); the supernatant was filtered through a 150 μm mesh and centrifuged again at 8000 g for 10 minutes. The pellet was resuspended in isolation buffer without BSA, centrifuged at 8000 g for 10 min and the final pellet resuspended in a small volume of isolation buffer and stored on ice until analysis. Protein concentration was determined by bicinchoninic acid (BCA) protein assay (Pierce) using bovine serum albumine as a standard. Mitochondria (0.4 mg protein/ml) were suspended in standard medium containing 250 mM sucrose, 1 mM KH_2PO_4, 20 μM EGTA, 10 mM MOPS, pH 7.4, and 5/2.5 mM glutamate/malate or 5 mM succinate (in the presence of 2 μM rotenone) as substrates. Oxygen consumption was determined fluorometrically, using a fiber optic oxygen sensor (Ocean Optics, Inc). Assays were performed at 37°C, on instruments equipped with thermostatic control and magnetic stirring.

Measurement of Isocitrate Dehydrogenase (IDH) Activity

Mitochondrial matrix was prepared from freshly isolated mitochondria by sonication (3 bursts for 10 seconds) and ultracentrifugation (43000 rpm for 30 min at 4˚C). $NADP^+$ dependent IDH activity was measured spectrophotometrically, following the reduction of $NADP^+$ at 340 nm and 37˚C in a buffer containing 33 mM KH_2PO_4, 1 mM CN^-, 1 mM $MgCl_2$, 1 mM $NADP^+$, pH 7.4. The reaction was initiated by the addition of 20 mM isocitrate. One unit of activity is defined as the production of 1 μmol NADPH min^{-1}. Protein concentration was determined by bicinchoninic acid (BCA) protein assay (Pierce), using BSA as a standard.

Statistical Analysis and Spot Selection Criteria

To address the issue of multiple comparisons and spurious associations, we considered controlling the family-wise error rate using the method of Bonferroni (dividing the type I error rate to declare statistical significance by the number of tests performed). However, Bonferroni correction was recently described to be "unduly strict" for this type of studies[12]. Therefore we also derived the q-values[13] from the calculated p-values, which allows for statistical inference with emphasis on the false discovery rate (that is, we can quantify the expected proportion of false positives among the spots declared significant). Statistically significant protein changes were determined using two-tailed student's t-tests of the normalized spot intensities between groups using a p value of less than 0.05. While none of the proteins spots reached statistical significance after a Bonferroni correction, the overall distribution of the p-values showed a very strong departure from a Uniform(0,1) distribution, which would have been expected under a global null (that is, no changes are observed in any of the proteins, Supplementary Figure 8). When controlling the false

discovery rate at 20%, a total of 76 spots are declared significant (of which we would expect approximately 15 to be false positives). Controlling the false discovery rate at a more stringent 10% still yields 28 significant spots (of which about 3 would be expected false positive). Thus, there is a large abundance of proteins that exhibit changes in concentration. The spots list, originally composed of over a hundred observations, was manually assessed to check for: consistency throughout the gels, signal saturation, MS identification susceptibility and mitochondrial localization, and therefore reduced to the final list presented in this study. Importantly, only protein changes $\geq$ 1.5-folds were considered to account for biological significance, after performing statistical analysis. Some of the changes (around one-third, $q \geq 0.2$) would not normally be considered signals but were retained because of the support of other biologically related changes (e.g. subunits of the same complex changing coherently or co-ordinated changes in known metabolic pathways). Few of them may require further validation and q-values are reported for clarity in Table 2. Indeed, none of these proteins (individually) reaches the statistical significance required after Bonferroni correction. This, obviously, is a consequence of the very small sample size, and the fact that about 1200 proteins were observed on the gels and had to be corrected for when attempting to control the family wise error rate (which is not very desirable in such a setting, as the p-values for true and false positives overlap substantially, due to the small sample size). Note that none of these considerations explicitly address the magnitude of the observed differences.

Supplemental Results

Differential Display Analysis

Table 2 lists protein changes in alphabetic order. The abundance of 31 protein species was changed in CRT group compared with DHF. MS identification, based on MS/MS, is listed. In a few cases, more than one protein was identified in a single gel spot, in most of these cases, carryover was ruled out based on spectra quality, number of unique peptides, and pI/MW values. In two cases it was not possible to unambiguously assign protein identity based on aforementioned criteria (eg. SAM50-like protein/ATP-synthase alpha subunit and NADH-dehydrogenase Fe-S 30 kDa/Clp protease) therefore multiple IDs are maintained in Figure 2H). Fold changes are presented with a positive or negative sign to indicate when their level were respectively increased or reduced upon CRT. Mitochondrial proteins are numbered, whereas mitochondria-associated proteins are marked with letters.

Other Protein Changes

The SAM50-like protein CGI-51 was detected together with ATPα in a protein spot that increased with CRT (3-fold, p=0.02,q=0.24). Although we could not unambiguously assign the protein spot identity, it is likely that ATPα, being a very highly abundant protein in mitochondria, is a carryover contaminant. Moreover the experimental pI and MW values are compatible with the assignment to SAM50 since ATPα theoretical pI is considerably different from the observed value.

Another spot is decreased in CRT (-2-fold, p0.031, q=0.27) and contains both the casein-like ATP-activated protease ClpP and the 30 kDa Fe-S subunit of complex I NADH-

dehydrogenase. Subsequent immunoblotting analysis confirmed a reduction in ClpP levels (see online Supplementary Figure 5 and Figure 2H in the main text).

Additionally, two proteins that are known to associate with mitochondria were found to be modulated by CRT were significantly altered upon CRT (Figure 2I of main text), Desmin, an intermediate filament protein that is known to interact with and influence mitochondrial function[14, 15], and GAPDH which interact with proteins on the cytosolic side of the outer mitochondrial membrane were increased in CRT (2- fold, p=0.003 and 0.02, and q=0.10 and 0.23 respectively).

ATPδ Subunit is Phosphorylated with CRT and DHF

Another subunit of complex V, ATP-synthase δ (ATPδ), displayed a change in pI upon treatment with alkaline phosphatase as shown in Supplementary Figure 1C of online supplement. The dominant blue colour (Cy2) of the basic spot indicates an increase in the density of the spot, corresponding to the un-phosphorylated form of ATPδ upon AP treatment. Phosphorylation of ATPδ was also confirmed through two-dimensional western blotting analysis using a specific antibody (anti-ATP5D, Atlas Antibody- Sigma). Supplementary Figure 1D shows a representative 2D western blotting of DHF, CRT and AP.

Ingenuity Pathways Analysis

FASTA sequences obtained from NCBI protein database listed in Table 2 were blasted against Uniprot database and the top ranking sequences were used to compile a dataset.

This also included the fold changes listed in Table 2. The dataset was up-loaded into IPA and a core analysis was performed. The canonical pathways that were modulated significantly according to the algorithm along with other major canonical pathways are displayed in Supplementary Figure 3.

Supplemental Discussion

Intriguingly, a membrane protein of unknown function, XP_53391 is strongly reduced in the CRT group. The biological role of this protein in the pathophysiology of HF has not yet been characterized suggesting a valuable new series of experiments to define its role. The C-terminus part of XP_53391 protein is homologous to the same portion of zebra fish isocitrate dehydrogenase gamma isoform (gi|62955395). IDH activity was tested, and found to have increased with CRT (Supplementary Figure 4). The XP_53391 protein spot decreased with CRT. Protein modification (see pI shift in Table 2) or different IDH protein isoform expression may explain this reverse correlation. However, further investigations are needed to assign IDH activity to XP 53391.

SAM50-like protein CGI-51 (sorting and assembly machinery component 50 homolog) was detected together with ATPα, in a spot whose quantity was increased by 3-fold in CRT. SAM50-like protein is poorly characterized and was found in the outer mitochondrial membrane of human heart mitochondria in association with the mitochondrial protein import machinery[16]. This evidence points to a potential increase in mitochondrial protein import capacity with CRT, in accordance with the observed reduction in protein turnover and improvement in mitochondrial protein synthesis.

We recently described a role for reduced apoptosis in the canine DHF model[3]. ROS production has been pointed as one of the possible causes for contractile deficiency and heart failure also based on their capacity to activate the mitochondrial apoptotic pathway[17, 18]. The remarkable increase in thioredoxin-dependent peroxide-reductase, found in the present study, suggests that the mitochondria in the CRT group are more protected against ROS production. Interestingly, another mitochondrial protein involved in redox protection and apoptosis regulation, programmed cell death 8 or apoptosis inducing factor (AIF), was elevated in the mitochondria obtained from CRT compared to DHF dogs. The role of AIF in oxidative stress protection and apoptosis is controversial[19]. However, increased susceptibility to oxidative stress and increased apoptosis after ischemia/reperfusion injury and aortic banding were reported in AIF-deficient mouse mutants (Harlequin, Hq) compared to wild type, confirming the function of AIF as a ROS scavenger in the heart, in vivo[20]. The contemporary increase in AIF levels observed in the present study, together with the reported reduced apoptosis in the same animal model, after CRT[3], support the hypothesis that AIF primary function in vivo is protection from ROS.

Finally, only few mitochondria-associated proteins were modified by CRT. The most important of these is desmin, that is the specific intermediate filament cytoskeleton protein in the cardiac myocyte and has shown the ability to modulate mitochondrial activity and localization [14, 15]. Mitochondrial localization is crucial in ensuring proper energy production and delivery to sites with high energy demand. Cytoskeletal and myofibrillar disarrangement in cardiac myocytes is one of the early features that define cardiac failure;

we believe that intermediate filaments play a crucial role in regulating the maladaptive transition to the diseased phenotype, possibly mediated by mitochondria re-distribution. It is therefore not surprising that this protein is changed when bi-ventricular pacing is applied.

Supplemental Figure Legends

Supplementary Figure 1. Succinate dehydrogenase and ATP-synthase δ subunit phosphorylation. Two representative images of de-phosphorylation 2DE zoomed at succinate dehydrogenase are shown for ease of comprehension: with three Cy Dyes is shown in panel A (DHF in green (Cy3), CRT in red (Cy5) and the alkaline phospatase-terated pool (AP) in blue (Cy2)); and the classical two-dyes de-phosphorylation assay described by Raggiaschi et al., in panel B. In panel C is presented the doublet obtained de-phosphorylation of ATPδ . Cy-dye sample and color- assignment are provided. In panel D a two-dimensional western-blotting analysis using a specific anti-ATPδ is also presented confirming pI shift upon tretment with AP. Note the shift in pI upon treatment with alkaline-phosphatase (AP). ☺; positive control for second dimension (SDS-PAGE).

Supplementary Figure 2. ATPβ degradation and MS/MS sequence coverage. Protein spots identified as ATPβ are indicated by arrows and accompanied by serial spot numbers (SSN) in Panel A. Panel B shows the sequence coverage obtained during the MS/MS abalysis for each individual spot. The sequence of the precursor protein (NCBI gi|73968432) is utilized, and the mitochondrial transit peptide adapted from the human sequence (47 aa, uniprot/swissprot database) is shown, together with its expected molecular weight. Bold red fonts indicate sequences covered by observed peptides. Red boxes

indicate the portion of the protein that is absent (i.e. not covered) in the specific protein fragment.

Supplementary Figure 3. Canonical pathways analysis through the Ingenuity Pathways Analysis (IPA) software. The ratio between the levels of protein in the CRT vs. DHF comparison are plotted along with a trend line (threshold) that divides the pathways that are significantly altered with CRT.

Supplementary Figure 4. Isocitrate activity in CRT and DHF hearts.

Supplementary Figure 5. Two-dimensional immunoblotting analysis for ClpP. The basic edge of 4-7 18 cm strip was cut and mounted on a small precast gel and subsequently blotted on PVDF. Anti-ClpP antibody (Sigma, Prestige Antibody, 1:2500 diluted) was used to probe the membrane. DHF, Dyssynchrony-induced Heart Failure; CRT, Cardiac Resynchronization Therapy; AP, alkaline phosphatase treatment.

Supplementary Figure 6. Experimental design and proteomics workflow. See main text for description. LBBB, left bundle branch blockade; TP, tachy-pacing; 2DE, two-dimensional electrophoresis; DHF, Dyssynchronous Heart Failure; CRT, Cardiac Resynchronization Therapy; AP, Alkaline Phosphatase; MS/MS, tandem mass spectrometry; IMAC, immobilized metal affinity chromatography.

Supplementary Figure 7. Mitochondrial enrichment protocol. Mitochondrial protein enrichment was evaluated by probing the fractions collected along with the enrichment protocol with specific antibodies for mitochondria (ATPβ) and myofilaments (Troponin I, TnI).

Supplementary Figure 8. Histogram of the protein p-values (A), and q-values for $p<0.05$ (B). The histogram shows a clear enrichment of low p-values, i.e. a strong departure from

a Uniform(0,1) distribution, which would be expected if no signal in the data existed. Q-values were calculated to address the multiple comparisons problem. The p-value cut-off for false discovery rate control at 10%, 20% and 30% were 0.003, 0.014, and 0.043, respectively. For example, declaring all differences with $p<0.013$ significant yields 62 spots, of which about 12-13 would be expected false positives.

Supplementary Figure 1

A.

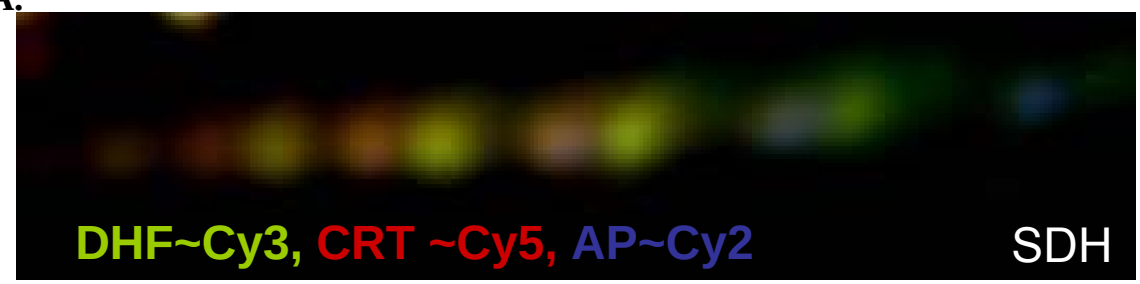

B.

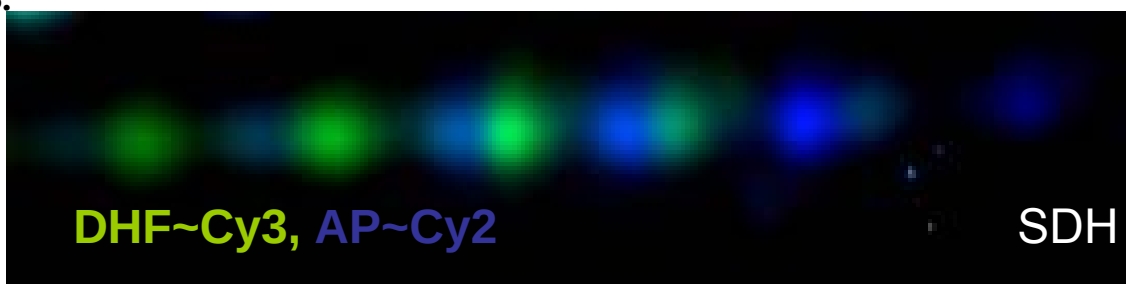

C.

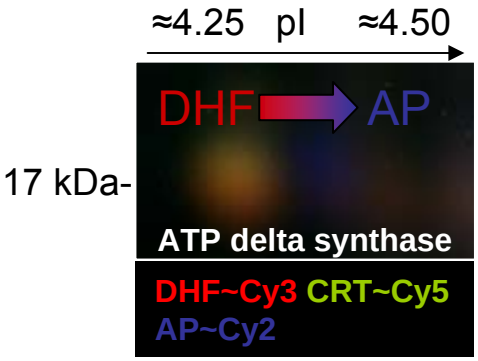

D.

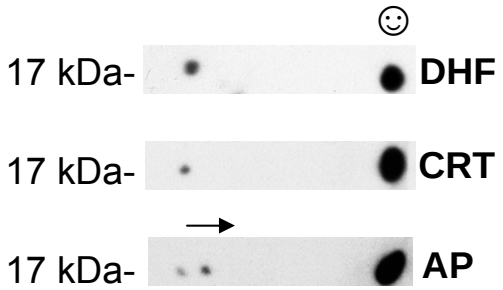

Supplementary Figure 2

A.

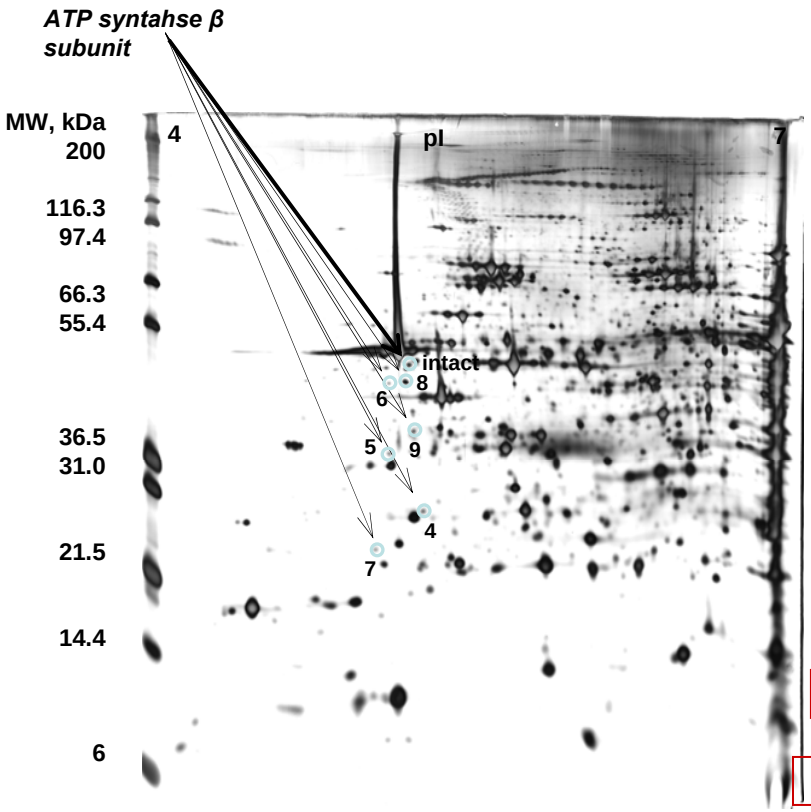

B.

{MATRIX SCIENCE} **Mascot Search Results**

Protein View

Match to: **gi|73968432** Score: **1526**
PREDICTED: similar to ATP synthase beta chain, mitochondrial precursor isoform 1 [Canis familiaris]
Found in search of C:\Xcalibur\data\Clients\VanEyk\AG\061016_vanEykJ_AG_D11.RAW

Nominal mass (M_r): **56250**; Calculated pI value: **5.21**
NCBI BLAST search of gi|73968432 against nr
Unformatted sequence string for pasting into other applications

Taxonomy: Canis familiaris

Fixed modifications: Carbamidomethyl (C)
Variable modifications: Oxidation (M)
Cleavage by Trypsin: cuts C-term side of KR unless next residue is P
Sequence Coverage: **36%**

Matched peptides shown in **Bold Red**

```
  1 MLGFVGRVAA TSASGALRGL GPSPLPQVKV LLRASPAALQ SARDYATQTS
 51 PSPKAGAATG RIVAVIGAVV DVQFDEGLPP ILNALEVQGR ETRLVLEVAQ
101 HLGESTVRTI AMDGTEGLVR GQKVLDSGAP IKIPVGPETL GRIMNVIGEP
151 IDERGPIKTK QFAAIHAEAP EFVEMSVEQE ILVTGIKVVD LLAPYAKGGK
201 IGLFGGAGVG KTVLIMELIN NVAKAHGGYS VFAGVGERTR EGNDLYHEMI
251 ESGVINLKDA TSKVALVYGQ MNEPPGARAR VALTGLTVAE YFRDQEGQDV
301 LLFIDNIFRF TQAGSEVSAL LGRIPSAVGY QPTLATDMGT MQERITTTKK
351 GSITSVQAIY VPADDLTDPA PATTFAHLDA TTVLSRAIAE LGIYPAVDPL
401 DSTSRIMDPN IVGNEHYDVA RGVQKILQDY KSLQDIIAIL GMDELSEEDK
451 LTVSRARKIQ RFLSQPFQVA EVFTGHMGKL VPLKETIKGF QQILAGEYDH
501 LPEQAFYMVG PIEEAVAKAD KLAEEHS
```

Intact, unphosphorylated

Transit peptide in human sequence UniProtKB/Swiss-Prot **P06576** (ATPB_HUMAN), ~5KDa

```
  1 MLGFVGRVAA TSASGALRGL GPSPLPQVKV LLRASPAALQ SARDYATQTS
 51 PSPKAGAATG RIVAVIGAVV DVQFDEGLPP ILNALEVQGR ETRLVLEVAQ
101 HLGESTVRTI AMDGTEGLVR GQKVLDSGAP IKIPVGPETL GRIMNVIGEP
151 IDERGPIKTK QFAAIHAEAP EFVEMSVEQE ILVTGIKVVD LLAPYAKGGK
201 IGLFGGAGVG KTVLIMELIN NVAKAHGGYS VFAGVGERTR EGNDLYHEMI
251 ESGVINLKDA TSKVALVYGQ MNEPPGARAR VALTGLTVAE YFRDQEGQDV
301 LLFIDNIFRF TQAGSEVSAL LGRIPSAVGY QPTLATDMGT MQERITTTKK
351 GSITSVQAIY VPADDLTDPA PATTFAHLDA TTVLSRAIAE LGIYPAVDPL
401 DSTSRIMDPN IVGNEHYDVA RGVQKILQDY KSLQDIIAIL GMDELSEEDK
451 LTVSRARKIQ RFLSQPFQVA EVFTGHMGKL VPLKETIKGF QQILAGEYDH
501 LPEQAFYMVG PIEEAVAKAD KLAEEHS
```

SSN 6

```
  1 MLGFVGRVAA TSASGALRGL GPSPLPQVKV LLRASPAALQ SARDYATQTS
 51 PSPKAGAATG RIVAVIGAVV DVQFDEGLPP ILNALEVQGR ETRLVLEVAQ
101 HLGESTVRTI AMDGTEGLVR GQKVLDSGAP IKIPVGPETL GRIMNVIGEP
151 IDERGPIKTK QFAAIHAEAP EFVEMSVEQE ILVTGIKVVD LLAPYAKGGK
201 IGLFGGAGVG KTVLIMELIN NVAKAHGGYS VFAGVGERTR EGNDLYHEMI
251 ESGVINLKDA TSKVALVYGQ MNEPPGARAR VALTGLTVAE YFRDQEGQDV
301 LLFIDNIFRF TQAGSEVSAL LGRIPSAVGY QPTLATDMGT MQERITTTKK
351 GSITSVQAIY VPADDLTDPA PATTFAHLDA TTVLSRAIAE LGIYPAVDPL
401 DSTSRIMDPN IVGNEHYDVA RGVQKILQDY KSLQDIIAIL GMDELSEEDK
451 LTVSRARKIQ RFLSQPFQVA EVFTGHMGKL VPLKETIKGF QQILAGEYDH
501 LPEQAFYMVG PIEEAVAKAD KLAEEHS
```

SSN 8

```
  1 MLGFVGRVAA TSASGALRGL GPSPLPQVKV LLRASPAALQ SARDYATQTS
 51 PSPKAGAATG RIVAVIGAVV DVQFDEGLPP ILNALEVQGR ETRLVLEVAQ
101 HLGESTVRTI AMDGTEGLVR GQKVLDSGAP IKIPVGPETL GRIMNVIGEP
151 IDERGPIKTK QFAAIHAEAP EFVEMSVEQE ILVTGIKVVD LLAPYAKGGK
201 IGLFGGAGVG KTVLIMELIN NVAKAHGGYS VFAGVGERTR EGNDLYHEMI
251 ESGVINLKDA TSKVALVYGQ MNEPPGARAR VALTGLTVAE YFRDQEGQDV
301 LLFIDNIFRF TQAGSEVSAL LGRIPSAVGY QPTLATDMGT MQERITTTKK
351 GSITSVQAIY VPADDLTDPA PATTFAHLDA TTVLSRAIAE LGIYPAVDPL
401 DSTSRIMDPN IVGNEHYDVA RGVQKILQDY KSLQDIIAIL GMDELSEEDK
451 LTVSRARKIQ RFLSQPFQVA EVFTGHMGKL VPLKETIKGF QQILAGEYDH
501 LPEQAFYMVG PIEEAVAKAD KLAEEHS
```

SSN 5

```
  1 MLGFVGRVAA TSASGALRGL GPSPLPQVKV LLRASPAALQ SARDYATQTS
 51 PSPKAGAATG RIVAVIGAVV DVQFDEGLPP ILNALEVQGR ETRLVLEVAQ
101 HLGESTVRTI AMDGTEGLVR GQKVLDSGAP IKIPVGPETL GRIMNVIGEP
151 IDERGPIKTK QFAAIHAEAP EFVEMSVEQE ILVTGIKVVD LLAPYAKGGK
201 IGLFGGAGVG KTVLIMELIN NVAKAHGGYS VFAGVGERTR EGNDLYHEMI
251 ESGVINLKDA TSKVALVYGQ MNEPPGARAR VALTGLTVAE YFRDQEGQDV
301 LLFIDNIFRF TQAGSEVSAL LGRIPSAVGY QPTLATDMGT MQERITTTKK
351 GSITSVQAIY VPADDLTDPA PATTFAHLDA TTVLSRAIAE LGIYPAVDPL
401 DSTSRIMDPN IVGNEHYDVA RGVQKILQDY KSLQDIIAIL GMDELSEEDK
451 LTVSRARKIQ RFLSQPFQVA EVFTGHMGKL VPLKETIKGF QQILAGEYDH
501 LPEQAFYMVG PIEEAVAKAD KLAEEHS
```

SSN 9

```
  1 MLGFVGRVAA TSASGALRGL GPSPLPQVKV LLRASPAALQ SARDYATQTS
 51 PSPKAGAATG RIVAVIGAVV DVQFDEGLPP ILNALEVQGR ETRLVLEVAQ
101 HLGESTVRTI AMDGTEGLVR GQKVLDSGAP IKIPVGPETL GRIMNVIGEP
151 IDERGPIKTK QLWAIHAEAP EFVEMSVEQE ILVTGIKVVD LLAPYAKGGK
201 IGLFGGAGVG KTVLIMELIN NVAKAHGGYS VFAGVGERTR EGNDLYHEMI
251 ESGVINLKDA TSKVTLVYGQ MNEPPGARAR VALTGLTVAE YFRDQEGQDV
301 LLFIDNIFRF TQAGSEVSAL LGRIPSAVGY QPTLATDMGT MQERITTTKK
351 GSITSVQAIY VPADDLTDPA PATTFAHLDA TTVLSRAIAE LGIYPAVDPL
401 DSTSRIMDPN IVGNEHYDVA RGVQKILQDY KSLQDIIAIL GMDELSEEDK
451 LTVSRARKIQ RFLSQPFQVA EVFTGHMGKL VPLKETIKGF QQILAGEYDH
501 LPEQAFYMVG PIEEAVAKAD KLAEEHS
```

SSN 8

```
  1 MLGFVGRVAA TSASGALRGL GPSPLPQVKV LLRASPAALQ SARDYATQTS
 51 PSPKAGAATG RIVAVIGAVV DVQFDEGLPP ILNALEVQGR ETRLVLEVAQ
101 HLGESTVRTI AMDGTEGLVR GQKVLDSGAP IKIPVGPETL GRIMNVIGEP
151 IDERGPIKTK QLWAIHAEAP EFVEMSVEQE ILVTGIKVVD LLAPYAKGGK
201 IGLFGGAGVG KTVLIMELIN NVAKAHGGYS VFAGVGERTR EGNDLYHEMI
251 ESGVINLKDA TSKVTLVYGQ MNEPPGARAR VALTGLTVAE YFRDQEGQDV
301 LLFIDNIFRF TQAGSEVSAL LGRIPSAVGY QPTLATDMGT MQERITTTKK
351 GSITSVQAIY VPADDLTDPA PATTFAHLDA TTVLSRAIAE LGIYPAVDPL
401 DSTSRIMDPN IVGNEHYDVA RGVQKILQDY KSLQDIIAIL GMDELSEEDK
451 LTVSRARKIQ RFLSQPFQVA EVFTGHMGKL VPLKETIKGF QQILAGEYDH
501 LPEQAFYMVG PIEEAVAKAD KLAEEHS
```

SSN 4

Supplementary Figure 3

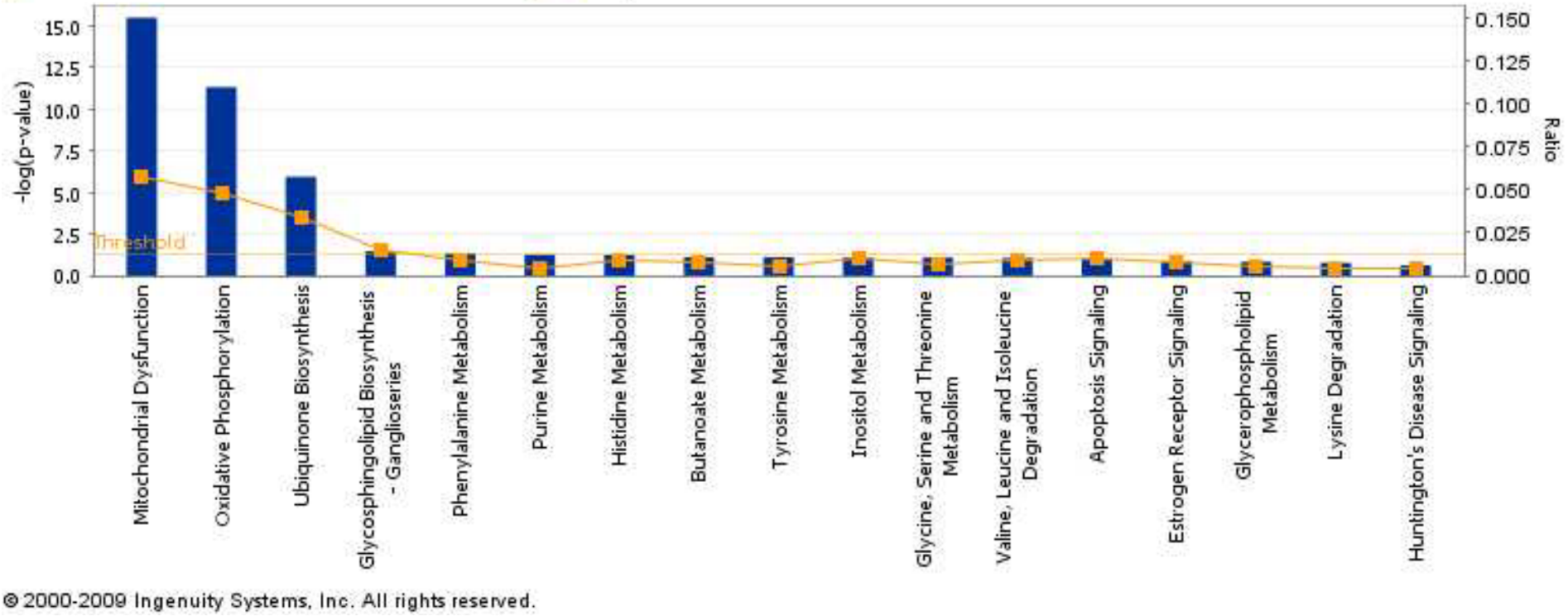

Supplementary Figure 4

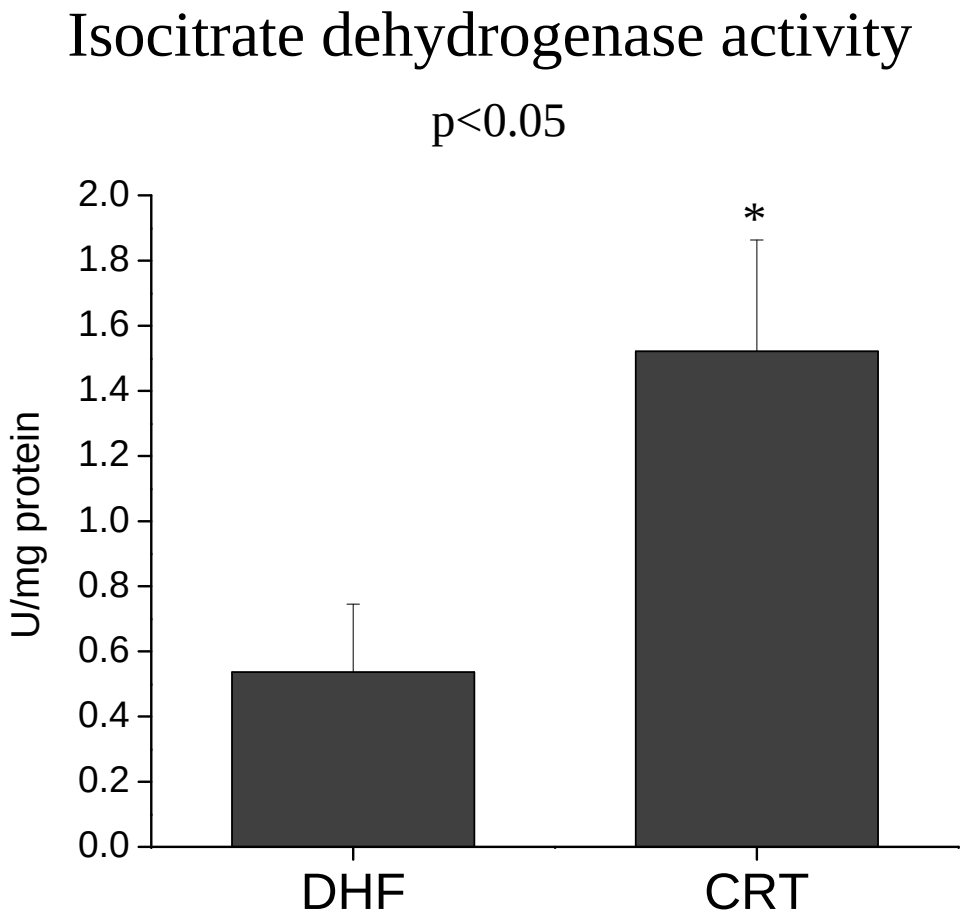

Supplementary Figure 5

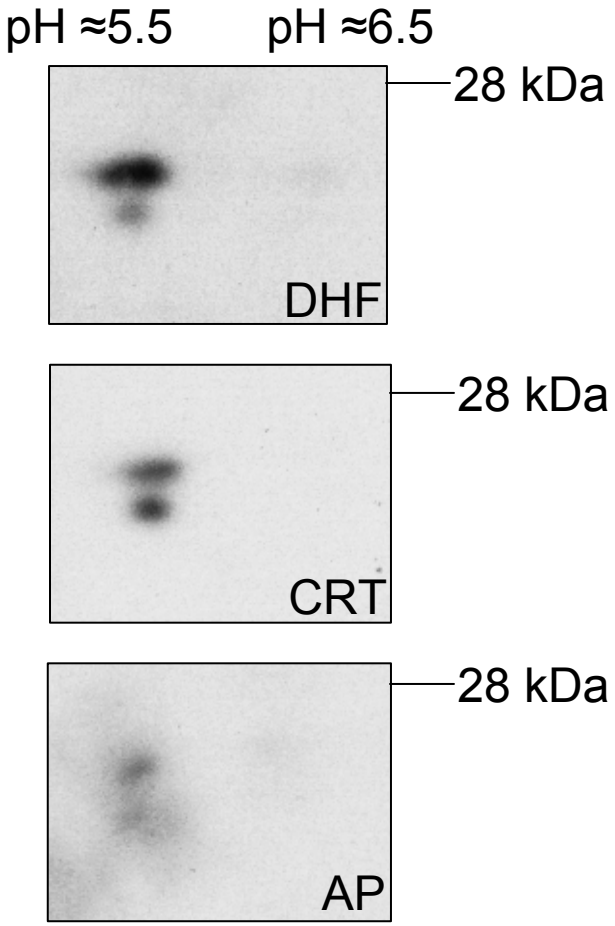

Supplementary Figure 6

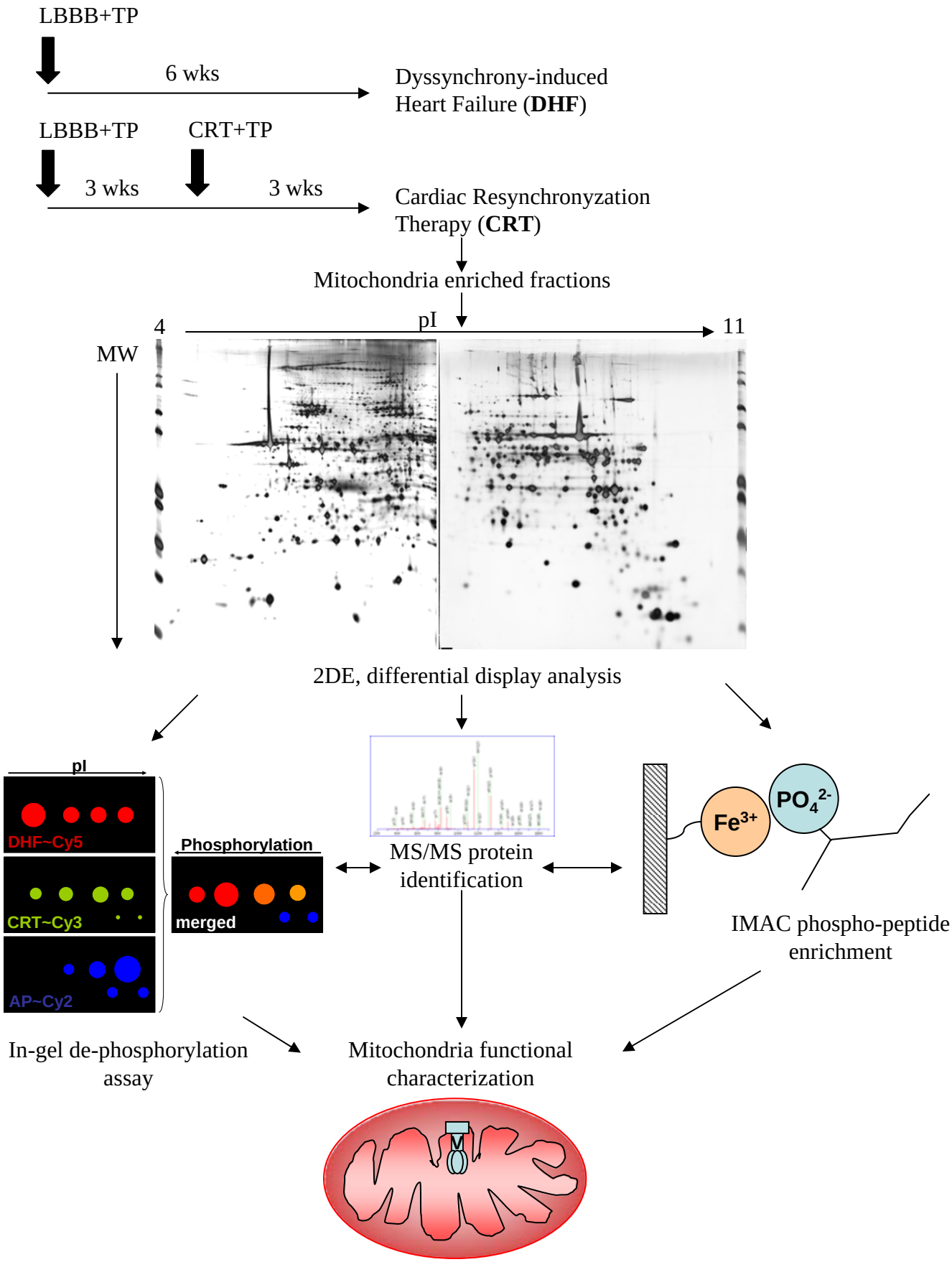

Supplementary Figure 7

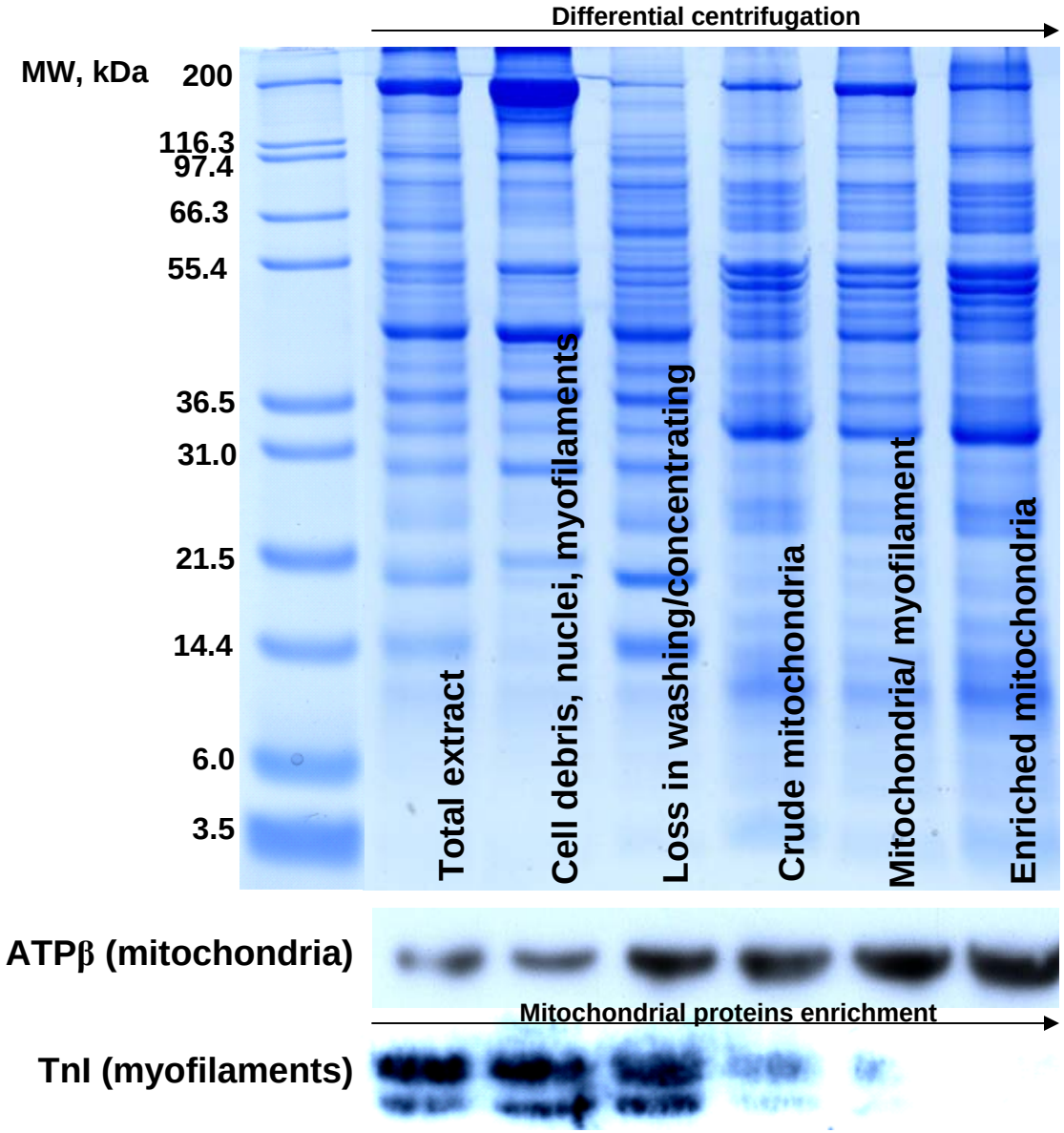

Supplementary Figure 8

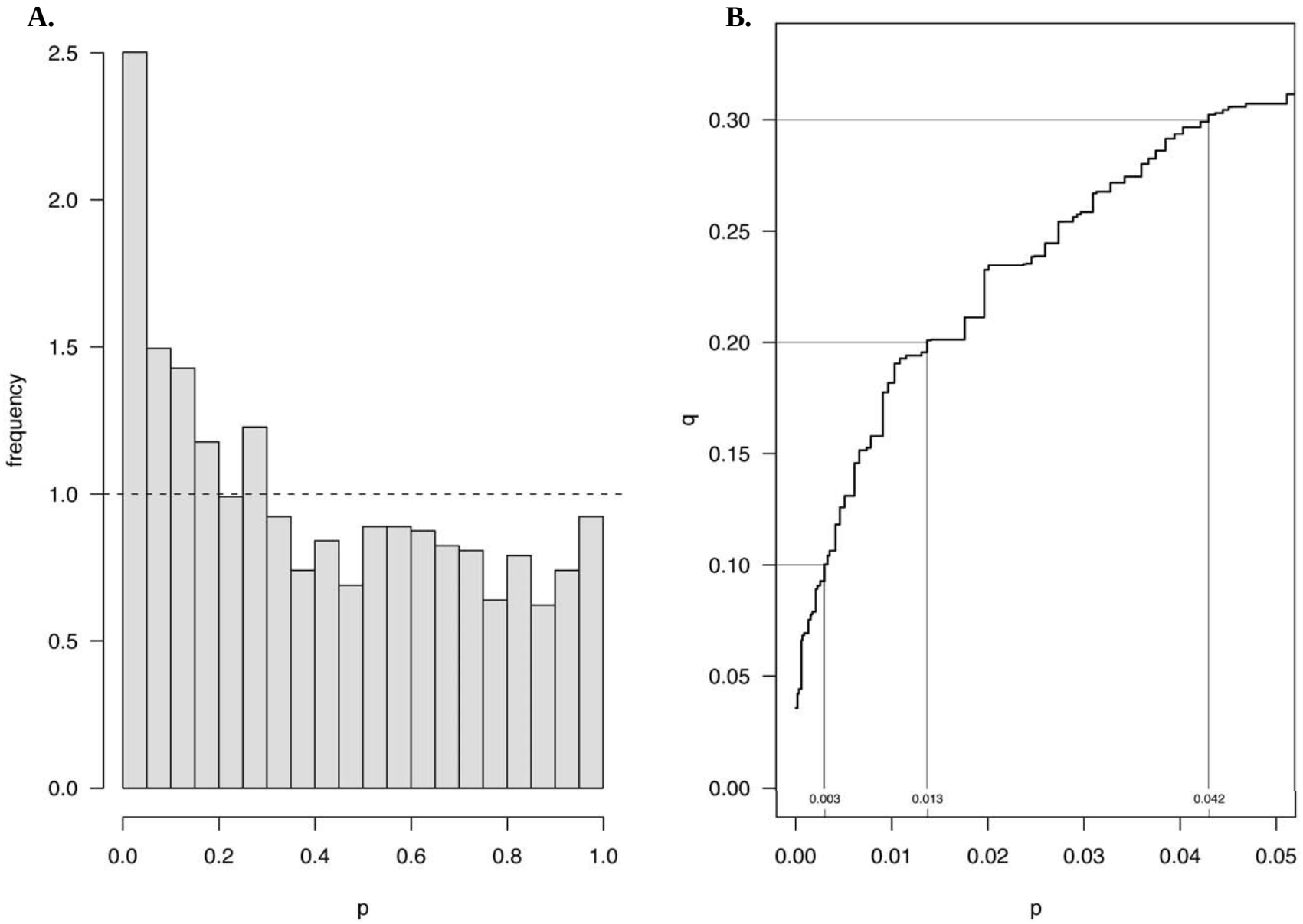

Supplemental References

1. Raggiaschi R, Lorenzetto C, Diodato E, Caricasole A, Gotta S, Terstappen GC. Detection of phosphorylation patterns in rat cortical neurons by combining phosphatase treatment and DIGE technology. *Proteomics.* 2006; 6: 748-756.

2. Matt P, Fu Z, Carrel T, Huso DL, Dirnhofer S, Lefkovits I, Zerkowski HR, Van Eyk JE. Proteomic alterations in heat shock protein 27 and identification of phosphoproteins in ascending aortic aneurysm associated with bicuspid and tricuspid aortic valve. *J Mol Cell Cardiol.* 2007; 43: 792-801.

3. Chakir K, Daya SK, Tunin RS, Helm RH, Byrne MJ, Dimaano VL, Lardo AC, Abraham TP, Tomaselli GF, Kass DA. Reversal of global apoptosis and regional stress kinase activation by cardiac resynchronization. *Circulation.* 2008; 117: 1369-1377.

4. Kane LA, Yung CK, Agnetti G, Neverova I, Van Eyk JE. Optimization of paper bridge loading for 2-DE analysis in the basic pH region: application to the mitochondrial subproteome. *Proteomics.* 2006; 6: 5683-5687.

5. Graham DR, Garnham CP, Fu Q, Robbins J, Van Eyk JE. Improvements in two-dimensional gel electrophoresis by utilizing a low cost "in-house" neutral pH sodium dodecyl sulfate-polyacrylamide gel electrophoresis system. *Proteomics.* 2005; 5: 2309-2314.

6. Shevchenko A, Wilm M, Vorm O, Mann M. Mass spectrometric sequencing of proteins silver-stained polyacrylamide gels. *Anal Chem.* 1996; 68: 850-858.

7. Gharahdaghi F, Weinberg CR, Meagher DA, Imai BS, Mische SM. Mass spectrometric identification of proteins from silver-stained polyacrylamide gel: a method for the removal of silver ions to enhance sensitivity. *Electrophoresis.* 1999; 20: 601-605.

8. Stastna M, Behrens A, Noguera G, Herretes S, McDonnell P, Van Eyk JE. Proteomics of the aqueous humor in healthy New Zealand rabbits. *Proteomics.* 2007; 7: 4358-4375.

9. Pappin DJ, Hojrup P, Bleasby AJ. Rapid identification of proteins by peptide-mass fingerprinting. *Curr Biol.* 1993; 3: 327-332.

10. Wilkins MR, Appel RD, Van Eyk JE, Chung MC, Gorg A, Hecker M, Huber LA, Langen H, Link AJ, Paik YK, Patterson SD, Pennington SR, Rabilloud T, Simpson RJ, Weiss W, Dunn MJ. Guidelines for the next 10 years of proteomics. *Proteomics.* 2006; 6: 4-8.

11. Bisetto E, Di Pancrazio F, Simula MP, Mavelli I, Lippe G. Mammalian ATPsynthase monomer versus dimer profiled by blue native PAGE and activity stain. *Electrophoresis.* 2007; 28: 3178-3185.

12. Kwong KS, Holland B, Cheung SH. A modified Benjamini–Hochberg multiple comparisons procedure for controlling the false discovery rate. *Journal of Statistical Planning and Inference.* 2002; 104: 351.

13. Storey JD. A direct approach to false discovery rates. *Journal of the Royal Statistical Society*. 2002; Series B: 479.

14. Capetanaki Y. Desmin cytoskeleton: a potential regulator of muscle mitochondrial behavior and function. *Trends Cardiovasc Med.* 2002; 12: 339-348.

15. Capetanaki Y, Bloch RJ, Kouloumenta A, Mavroidis M, Psarras S. Muscle intermediate filaments and their links to membranes and membranous organelles. *Exp Cell Res.* 2007; 313: 2063-2076.

16. Xie J, Marusich MF, Souda P, Whitelegge J, Capaldi RA. The mitochondrial inner membrane protein mitofilin exists as a complex with SAM50, metaxins 1 and 2, coiled-

coil-helix coiled-coil-helix domain-containing protein 3 and 6 and DnaJC11. *FEBS Lett.* 2007; 581: 3545-3549.

17. Byrne JA, Grieve DJ, Cave AC, Shah AM. Oxidative stress and heart failure. *Arch Mal Coeur Vaiss.* 2003; 96: 214-221.

18. Takimoto E, Kass DA. Role of oxidative stress in cardiac hypertrophy and remodeling. *Hypertension.* 2007; 49: 241-248.

19. Porter AG, Urbano AG. Does apoptosis-inducing factor (AIF) have both life and death functions in cells? *Bioessays.* 2006; 28: 834-843.

20. van Empel VP, Bertrand AT, van der Nagel R, Kostin S, Doevendans PA, Crijns HJ, de Wit E, Sluiter W, Ackerman SL, De Windt LJ. Downregulation of apoptosis-inducing factor in harlequin mutant mice sensitizes the myocardium to oxidative stress-related cell death and pressure overload-induced decompensation. *Circ Res.* 2005; 96: e92-e101.